Superconductivity of strongly correlated systems / Supraconductivité des systèmes fortement corrélés

Properties of ferromagnetic superconductors

Des supraconducteurs ferromagnétiques

Dai Aoki [a,*], Frédéric Hardy [b], Atsushi Miyake [a,c], Valentin Taufour [a], Tatsuma D. Matsuda [a,d], Jacques Flouquet [a]

[a] SPSMS, UMR-E CEA / UJF-Grenoble 1, INAC, 38054 Grenoble, France
[b] Karlsruhe Institut für Technologie, Institut für Festkörperphysik, 76021 Karlsruhe, Germany
[c] KYOKUGEN, Osaka University, Toyonaka, Osaka 560-8531, Japan
[d] Advanced Science Research Center, Japan Atomic Energy Agency, Tokai, Ibaraki 319-1195, Japan

A B S T R A C T

Thanks to the discovery in the last decade of three uranium ferromagnetic superconductors, UGe$_2$, URhGe and UCoGe, the fascinating aspects of the interplay between the triplet state of Cooper pairing and ferromagnetism have emerged. Furthermore, as the ferromagnetic properties in the normal state are quite different with respect to the proximity of the ferromagnetic–paramagnetic instabilities, the feedback with the coexistence of super-conductivity gives rise to quite different boundaries in pressure and magnetic field. Special attention is given on the location of the materials with respect to the tricriticality and on the reinforcement of SC in a transverse field response with respect to the direction of the FM sublattice magnetization. The other facts of the interplay between FM and SC is briefly mentioned.

© 2011 Académie des sciences. Published by Elsevier Masson SAS. All rights reserved.

R É S U M É

La découverte cette dernière décade de trois supraconducteurs ferromagnétiques (UGe$_2$, URhGe, UCoGe) a permis de réaliser des études sur deux états principaux de la matière condensée : la supraconductivité et le ferromagnétisme. La conséquence de la condensation en paire de Cooper de quasiparticules issus d'un ferromagnétisme itinérant se signale par leur appariement en triplet. Comme l'état ferromagnétique de ses trois systèmes diffère fortement par rapport à la proximité de l'instabilité ferromagnétique–paramagnétique, leur diagramme de phase en champ magnétique et en pression va démontrer une grande diversité. Dans le cas de UGe$_2$, l'accent est mis sur les conséquences de balayer en pression le point tricritique ferromagnétique puis de voir jusqu'à quel champ magnétique longitudinal la restauration en champ longitudinal du ferromagnétisme disparaît. Dans le cas de deux autres composés, l'effet spectaculaire, lié à l'affaiblissement du ferro-magnétisme, est celui d'un champ magnétique transverse qui, renforçant la masse effective des quasiparticules, magnifie les propriétés supraconductrices. L'état du domaine est décrit tant d'un point de vue expérimental que théorique.

© 2011 Académie des sciences. Published by Elsevier Masson SAS. All rights reserved.

* Corresponding author.
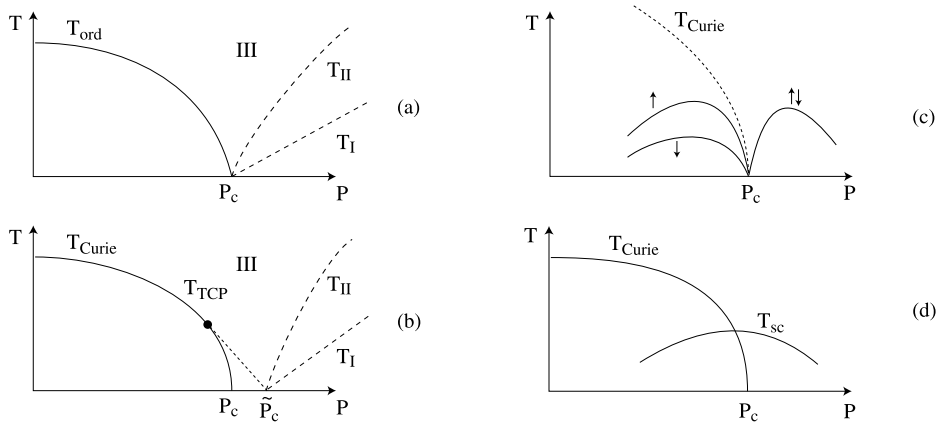*E-mail address:* Dai.Aoki@cea.fr (D. Aoki).

Fig. 1. (a) Magnetic phase diagram from the SCR theory. Below T_I, the Fermi liquid properties are observed. For a first-order transition, P_c can reach $\tilde{P}_c$ if $\triangle M_0$ is close to zero (b). (c) Superconducting phase diagram near the ferromagnetic instability, from Fay and Appel. (d) Phase diagram of UCoGe.

Table 1
Pressure dependence of T_I, T_{II}, T_{Curie} and the relation between the sublattice magnetization M_0 and T_{Curie} for 3D FM systems.

	T_I	T_{II}	T_{II}/T_I	T_{Curie}	$T_{Curie}(M_0)$
FM	$(P - P_c)^{3/2}$	$(P - P_c)^{3/4}$	$(P - P_c)^{-3/4}$	$(P - P_c)^{3/4}$	$M_0^{3/2}$

1. Introduction

The discovery of superconductivity (SC) in the ferromagnet UGe_2 has opened a new chapter in the exotic domain of unconventional superconductivity [1]. The trend is that the ferromagnetic (FM) interaction between highly renormalized quasiparticles is the source of SC pairing. In the three Ising ferromagnetic superconductors UGe_2, URhGe [2] and UCoGe [3], it appears that the Cooper pairs condense in the equal spin pairing state (ESP) with $\uparrow\uparrow$ and $\downarrow\downarrow$ spin carriers. In this review, we give a schematic view of the phenomenon. This article is quite complementary to the paper recently published in J. Phys. Soc. Jpn. for the 100 years of superconductivity [4]. We focus on temperature (T), pressure (P) and magnetic field (H) phase diagrams, in particular on the precise location of the FM and FM + SC phases, and the PM (paramagnetic) and PM + SC boundaries. In these compounds, the occurrence of SC is strongly related to the effective mass enhancement associated with the ferromagnetic instability which occurs in UCoGe at the critical point (P_c, $T = 0$) where FM is collapsed, while in UGe_2 two distinct ferromagnetic phases FM1 and FM2 are separated by P_x. The new feature of these Ising ferromagnets is that the field response of the FM–PM instability is quite anisotropic between $H \parallel M_0$ and $H \perp M_0$, where M_0 is the sublattice magnetization. Furthermore, when the system moves towards P_c, the FM–PM transition line, $T_{Curie}(P)$, becomes first order and the occurrence of tricriticality at (T_{TCP}, P_{TCP}) leads to the existence of a field induced FM phase which extends beyond P_c till a quantum critical end point (QCEP) at (P_{QCEP}, H_{QCEP}).

In this article, first we briefly describe the features of itinerant ferromagnetism and SC pairing mediated by ferromagnetic fluctuations and then we summarize the normal-state properties of UGe_2, URhGe and UCoGe and comment on their influence on the appearance of SC at zero field. We discuss the occurrence of tricriticality in UGe_2 and the H reinforced/reentrant SC for $H \perp M_0$ in URhGe and UCoGe in the context of their longitudinal and transverse field responses [5–7]. In conclusion, we give a short list of other aspects of the interplay between FM and SC.

2. Ferromagnetism in itinerant electronic system

A major breakthrough in the understanding of FM in itinerant systems appeared in 1985 with Moriya's self-consistent renormalization (SCR) theory of spin fluctuations in a Hubbard scheme. In this model, the Fermi liquid regime, which is characterized by a specific-heat linear term γ and a T^2 dependent resistivity below a temperature T_I, collapses when the transition from a long range FM order to a PM ground state occurs at a characteristic pressure P_c. On the other hand, the non-Fermi liquid (NFL) regime between T_I and T_{II} expands before recovering a high temperature domain T_{III} (see Fig. 1(a)) [8,9]. Pressure often tunes the system from FM to PM since it increases the electronic bandwidth W and thus decreases the density of states $N(\varepsilon_F)$. Below P_c, $UN(\varepsilon_F)$ is larger than 1 while above P_c, $UN(\varepsilon_F)$ is smaller than 1, where U is the onsite Coulomb repulsion and $N(\varepsilon_F)$ is the electronic density of state at the Fermi level. Table 1 summarizes the expected P dependence of T_I, T_{II} and T_{Curie} together with the variation of T_{Curie} with M_0.

Below T_I, the effective mass m^* taken from $\gamma \sim m^* k_F$ diverges as $\log(P - P_c)$, while the uniform susceptibility $\chi(0)$ and the resistivity inelastic term A diverge as $\frac{1}{P - P_c}$ (Table 2). In addition, the temperature variation of C/T and $\chi(0)$ and the exponent n of the resistivity term depend on the magnetic dimensionality as shown in Table 3. However, there is

Table 2
Pressure dependence of γ, $\chi_{Q=0}$ and A near P_c for 3D FM systems.

	γ	$\chi_{Q=0}$	A
FM	$\log(P - P_c)$	$(P - P_c)^{-1}$	$(P - P_c)^{-1}$

Table 3
Temperature variation of C/T, $\chi_{Q=0}$ and resistivity for 3D and 2D FM systems.

	C/T	$1/\chi_{Q=0}$	$\rho \sim T^n$
FM 3D	$-\log T$	$T^{4/3}$	$T^{5/3}$
FM 2D	$T^{-1/3}$	$-T \log T$	$T^{4/3}$

a major difference between FM and antiferromagnetic (AFM) quantum critical points. For the latter no divergence of m^* occurs at P_c and γ varies as $\gamma_0(P - P_c)^{1/2}$. The $(P - P_c)^{1/2}$ singularity leads to a divergence of the Grüneisen parameter $\Omega_e = -\partial \log \gamma / \partial \log V$ at P_c. For a second-order phase transition, both the entropy (S) and the thermal expansion ($\partial S / \partial P$) collapse at P_c (Fig. 1(a)).

For FM systems, it is well established both experimentally [10] and theoretically [11] that the divergence of m^* at P_c is inhibited by the occurrence of a first-order transition at P_c (Fig. 1(b)) which is characterized by discontinuities ΔM_0, ΔV_0 in M_0 and volume V_0, respectively. As the entropy reaches zero at $P = P_c$ according to the Clausius–Clapeyron relation ($dP/dT = \Delta S / \Delta V$), the initial (T, P) line at very low temperature must be vertical. If ΔM_0 is small, the quantum phase transition at P_c will only be weakly first-order and strong fluctuations will persist, being almost like the second-order phase transition. Thus for a strong first-order transition (large ΔM_0 and large ΔV) there is a large difference between P_c and $\tilde{P}_c$.

The SCR theory was developed for 3D itinerant magnets and extended to the case of heavy fermion systems (HFS) with the simple idea that the bandwidth W is renormalized to a Kondo energy $k_B T_K$ characteristic of the strong local nature of the magnetism and its fluctuations [12]. This leads to a strongly renormalized band mass m_B and a further enhancement of m^{**} due to the FM quasiparticle interactions [13]. Very often m_B and m^{**} have comparable amplitudes. Thus, the image of interfering quasiparticles is that of interfering waves with a large diffraction pattern given by the strong local character of the magnetism.

In the case of cerium HFS, the effect of pressure is to switch the system from a magnetically ordered state to a PM ground state. This is due to the strong P increase of the Kondo energy $k_B T_K$ in comparison with the indirect intersite coupling, given by the Ruderman, Kittel, Kasuya, Yosida (RKKY) interaction. Pressure drives the Ce systems from a trivalent configuration (with a $4f$-shell occupation number $n_f \sim 1$) to a tetravalent configuration with $n_f \sim 0$. According to the $4f$ electron–hole symmetry, n_f can vary from $n_f = 14$ (Yb^{2+}) to $n_f = 13$ (Yb^{3+}) in ytterbium HFS and magnetic ground states appear under pressure [9]. For uranium compounds, it is difficult to predict the pressure dependence of T_{Curie} because the fluctuations now occur between the two magnetic configurations U^{3+} and U^{4+}.

3. Cooper pairing and ferromagnetism

Soon after the elaboration of the BCS theory of s-wave superconductivity, [14] the problem of coexistence of SC and FM was discussed by V. Ginzburg. He noticed that finding SC in ferromagnets is as probable as finding non-ferromagnetic SC in large magnetic fields [15]. However, the relevance of FM spin fluctuations for SC was pointed out in 1966 [16]. The existence of an anisotropic BCS state was illustrated by the p-wave superfluidity observed in liquid ^{3}He [17–19]. p-wave SC transitions for paramagnon mediated SC in nearly FM systems were first calculated by Layzer and Fay in 1971 [20]. However, it is only in 1980 that Fay and Appel published the first paper concerning the variation of T_{sc} through P_c in the limited context of the so-called equal spin pairing (ESP) state with $\uparrow\uparrow$ and $\downarrow\downarrow$ quasiparticles (Fig. 1(b)) [21]. The ESP interaction with $\uparrow\uparrow$ and $\downarrow\downarrow$ components of the triplet channel with an angular momentum q is related to the non-interacting Lindhard response of the spin $\chi_0^{\uparrow}$ and $\chi_0^{\downarrow}$ by the relation:

$$V_{\uparrow\uparrow} = \frac{\Delta^2 \chi_0^{\downarrow}}{1 - U^2 \chi_0^{\downarrow}(q) \chi_0^{\uparrow}(q)} \tag{1}$$

To mediate SC with a $\uparrow\uparrow$ minority-spin component, a majority-spin component $\downarrow\downarrow$ is required. As shown in Fig. 1(b), the $\uparrow\uparrow$ minority-spin carriers first condense in the FM state and SC corresponds to a two-band model. In the PM region, both components condense at the same critical temperature. However, if FM abruptly disappears through a first-order transition at P_c instead of $\tilde{P}_c$, it is then clear that the singularity at P_c could be suppressed (Fig. 1(b)).

In the theory of Fay and Appel performed for the second-order transition, the superconducting critical temperature T_{sc} is described by

$$T_{sc} = \omega_c \exp\left(-\frac{1 + \lambda_z}{\lambda_{\Delta}}\right) \tag{2}$$

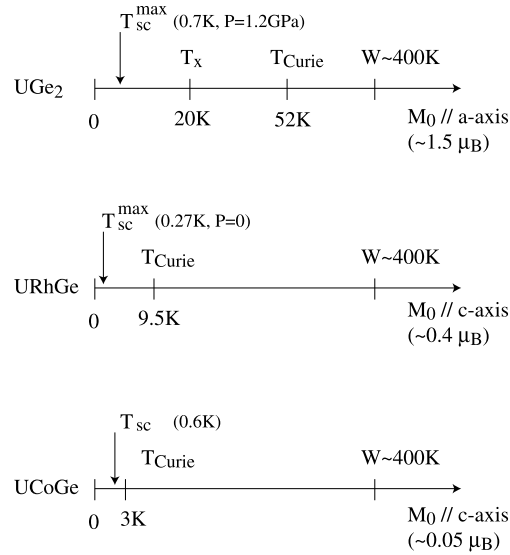**Fig. 2.** Characteristic energy scales of the three ferromagnetic superconductors, UGe_2, URhGe and UCoGe.

where λ_z is the renormalized-mass parameter and λ_Δ is the interaction parameter. ω_c, which is basically proportional to T_I, vanishes at P_c. Close to P_c, this formula differs from the well-known McMillan-like formula,

$$T_{sc} \sim T_0 \exp(-1/\lambda) \tag{3}$$

with

$$\lambda = \frac{\lambda_\Delta}{1 + \lambda_z} \tag{4}$$

and where T_0 is a characteristic cutoff energy. Outside around P_c, they are basically the same. For URhGe, a simpler expression was chosen, [13]

$$T_{sc} \sim T_0 \exp\left(-\frac{m^*}{m^{**}}\right) \tag{5}$$

$$m^* = m_B + m^{**} \tag{6}$$

where the quasiparticle effective mass m^* is the sum of the band mass m_B and the correlation mass m^{**}. Here $1 + \lambda_z = m^*/m_0$ and $\lambda_\Delta = m^{**}/m_0$, where m_0 is the free electron mass. Further calculations of $T_{sc}(P)$ show that T_{sc} has only weak minima at P_c [22]. Additional discussions concerning the coexistence of FM and SC can be found in Refs. [23–28]. Calculations in the PM side of P_c, for AF and FM interactions, were performed using the Eliashberg formalism for the quasi-2D and 3D cases [29] with specific applications to cubic and tetragonal symmetries as a function of the electronic or magnetic anisotropy [30]. In general, a spin singlet is favored. However, for a triplet state, pairing is only caused by longitudinal fluctuations whereas transverse fluctuations are pair-breaking and impurity scattering is strongly enhanced at P_c [31]. Thus, it is not surprising that triplet SC in ferromagnets has only been discovered in Ising ferromagnets. Finally, the possible SC order parameters in ferromagnetic materials have been classified using general symmetry arguments for cubic and orthorhombic structures [32–34].

4. Three ferromagnetic superconductors: UGe_2, URhGe and UCoGe

SC was discovered in the three uranium ferromagnets UGe_2, URhGe and UCoGe where a strong $5f$ electronic component exists at the Fermi energy in the density of states. Thus, the $5f$ electrons are strongly delocalized. Fig. 2 summarizes their main characteristic parameters. For UGe_2, FM appears at a rather high temperature, $T_{Curie} \sim 52$ K, which is quite comparable to the renormalized bandwidth W. The existence of the Fermi surface will be felt below $T \sim W/10$. At ambient pressure the specific heat exhibits a clear jump at T_{Curie}, as shown in Fig. 3(a) [35]. At $T_x \sim 25$ K, a crossover occurs between two interfering FM phases; FM2 with a sublattice magnetization $M_0 \approx 1.5\mu_B$ and FM1 with $M_0 \approx 1\mu_B$ [36]. SC appears only under pressure with a maximum $T_{sc}^{max} \sim 0.7$ K, at the pressure $P_x \sim 1.2$ GPa, where the ground state switches from FM2 to FM1 [37]. A clear specific-heat anomaly was detected at $T_x(P)$ for $P \sim P_x$ [38]. Finally, FM disappears at $P_c \sim 1.49$ GPa.

URhGe with $T_{Curie} = 9.5$ K is of great experimental interest because it becomes superconducting with $T_{sc} = 0.27$ K at ambient pressure (Fig. 3(b)). Thus, it offers the possibility of applying a larger variety of experimental methods for understanding its superconducting properties. T_{Curie} appears well below the characteristic temperature related to the bandwidth (W).
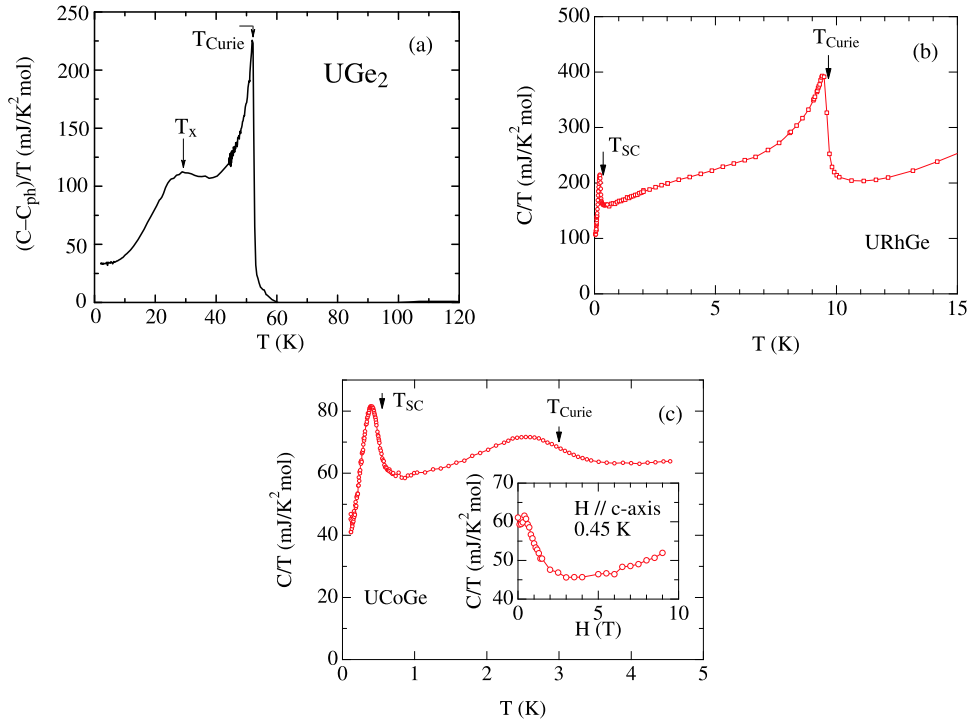
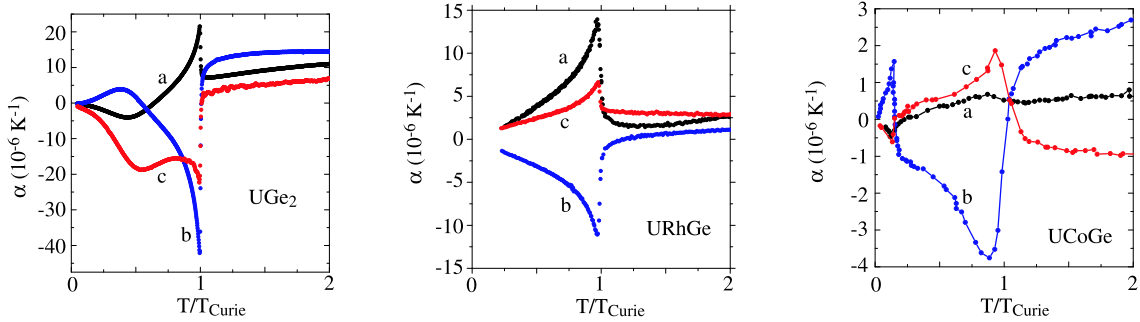**Fig. 3.** Specific heat of UGe$_2$, URhGe and UCoGe. The phonon contribution is subtracted for UGe$_2$ [35,39,7].

Fig. 4. Temperature dependence of the thermal-expansion coefficients along a-, b- and c-axis in UGe$_2$, URhGe and UCoGe [35,39,47].

The low-temperature Sommerfeld coefficient is equal to 160 mJ/K^2 mol [7,39]. With increasing pressure, T_{Curie} increases while T_{sc} decreases [40]. Thus, URhGe can be considered as a good example of the interplay between SC and FM which is far from the critical regime around P_c.

Again, T_{Curie} is much lower than W in UCoGe. However, the specific heat anomaly at $T_{\mathrm{Curie}} \sim 3$ K, shown in Fig. 3, is very broad and highly dependent on the sample purity. In fact, there is evidence from NMR measurements that the transition is indeed first order [41] and the specific-heat anomaly results from the discontinuous change in entropy at T_{Curie} and strong fluctuations, which indicate that the magnetic coherence length remains constant over an extended T window. UCoGe is a unique example of ferromagnetic superconductivity at ambient pressure with a rather small ordered moment $M_0 \sim 0.05\mu_{\mathrm{B}}$. With increasing pressure, T_{Curie} decreases and vanishes at P_c while T_{sc} initially raises and exhibits a broad maximum at P_c [42–44]. Another unique feature of UCoGe is its low carrier concentration which implies that the contribution of the Co 3d states to the density of states is not negligible at the Fermi energy [45,46].

As these compounds all have an orthorhombic structure, it is interesting to study their thermal-expansion coefficients along the three principal axes a, b and c [35,39,47,7] which are related to the uniaxial pressure derivative of T_{Curie} via the Ehrenfest and Clausius–Clapeyron relations for second-order and first-order transitions, respectively. As illustrated in Fig. 4, the thermal-expansion coefficients along the three axes do not show the same variation with uniaxial pressure at T_{Curie}. For these three compounds, a large negative drop of α_b is observed at T_{Curie}. It must be noted that for UGe$_2$, the crossover regime at $T_x \sim 25$ K from FM1 to FM2 is marked by extrema in α_a, α_b and α_c which do not coincide in position. Above the critical pressure P_c, where the system switches from FM1 to FM2 through a real first-order transition, the jumps measured
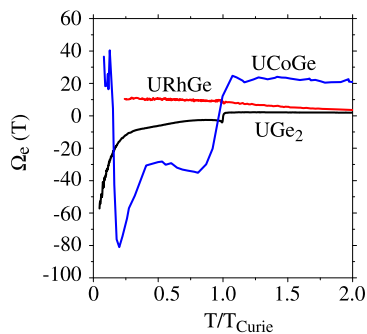
Fig. 5. Temperature dependence of the Grüneisen parameter in UGe$_2$, URhGe and UCoGe [39].
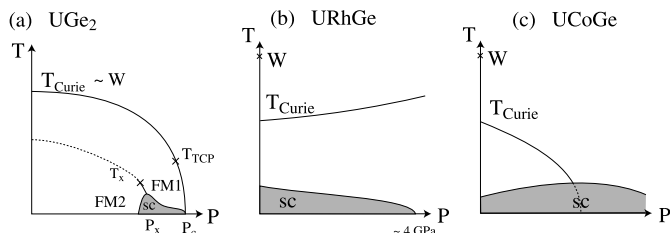

Fig. 6. Schematic (T, P) phase diagrams of UGe$_2$, URhGe and UCoGe.

along the three axis have to occur at the same temperature [48]. In UCoGe, the thermal expansion was also measured below T_{sc}. The volume changes at T_{Curie} and T_{sc} are opposite in sign, as observed in other highly anisotropic materials like URu$_2$Si$_2$ where the volume changes at the hidden order transition and T_{sc} are opposite in sign, as well.

The ratio of the volume thermal-expansion coefficient to the specific heat gives the opportunity to calculate the electronic Grüneisen parameter $\Omega_e(T)$, as shown in Fig. 5. Above T_{Curie}, the three compounds have a positive Grüneisen coefficient: the pressure derivative of the entropy, dS/dP is negative. For URhGe, this sign remains the same on cooling through T_{Curie} since T_{Curie} increases with pressure. However, a sharp sign change occurs for UCoGe and UGe$_2$ (dS/dP becomes positive) in excellent agreement with the observation that T_{Curie} collapses at 1 GPa and 1.5 GPa in UCoGe and UGe$_2$, respectively. In UGe$_2$, it is interesting to remark that T_{Curie} is comparable to W and that the electronic Grüneisen parameter in the PM phase is quite close to zero. For UCoGe, $\Omega_e(T)$ is already large and temperature independent above T_{Curie} with a value quite similar to that of the intermediate valence Ce compounds.

5. (T, P) phase diagram: interplay of SC, PM and FM

Fig. 6 shows schematic (T, P) phase diagrams of UGe$_2$, URhGe and UCoGe. In UGe$_2$, SC is squeezed between the two first-order transitions at P_x and P_c [1,37,49]. The robust first-order nature of these transitions makes it difficult to establish whether SC exists homogeneously in the FM2 and PM phases and a definite conclusion is still under debate. Furthermore, the Fermi surface changes between the FM2 and the PM states [50,51]. Two different models were proposed to explain the maximum of T_{sc} at P_x. In the first one, SC is mediated by the charge density wave or spin density wave (CDW/SDW) fluctuations at P_x [52] while the second one invokes a twin-peak structure in the electronic density of states [53]. No extra superstructures were observed at P_x. The transition from FM2 to FM1 seems restricted to a switch between two FM states with consequences on λ_z and λ_Δ reproducing rather well the pressure variation of T_{sc}.

In URhGe, the situation corresponds to the behavior predicted in the FM domain for $P \ll P_c$ with the particularity that T_{Curie} increases with P while T_{sc} decreases and disappears above 4 GPa (Fig. 6(b)) [40,54].

In UCoGe, T_{Curie} and T_{sc} tend to merge with increasing pressure [42,44] and the FM anomaly is no longer detected in resistivity and susceptibility measurements when $T_{sc} \approx T_{Curie}$. Thus, T_{Curie} seems to collapse suddenly under pressure leaving a wide maximum in the pressure dependence of T_{sc}. At least, the observation of the SC anomaly in the PM side indicates that bulk superconductivity exists in the PM domain [43].

6. Longitudinal and transverse magnetic field response

In these Ising ferromagnets, the magnetic field leads to a particular response when it is applied either parallel or perpendicular to the initial sublattice magnetization M_0 (oriented along the a axis for UGe$_2$ and along the c axis for URhGe and UCoGe).

In UGe$_2$, the FM transition at T_{Curie} at ambient pressure is of second order and the application of a magnetic field parallel to M_0 weakens the FM correlations. Thus, the FM specific-heat anomaly is rapidly reduced and shifts to higher temperature with increasing H; T_{Curie} seems to increase with H but γ reaches the band-mass value γ_B when the field strength is comparable to the molecular field. In UGe$_2$, this molecular field is very large ~ 200 T.

However, the nature of the transition at T_{Curie} changes under pressure from second to first order at the tricritical point (T_{TCP}, P_{TCP}) [55,56]. When the field is applied along the sublattice magnetization M_0, the occurrence of this tricriticality gives rise to in-field FM wings that open at the TCP and terminate at quantum critical end-points located at (P_{QCEP}, H_{QCEP}) for $T = 0$ (see Fig. 7). The pressure difference $P_{QCEP} - P_c$ is related to the pressure difference $\tilde{P}_c - P_c$ which correlates with the jump ΔM_0 observed at P_c. UGe$_2$ represents an ideal case for studying FM tricriticality since $\Delta M_0 \sim 0.9 \mu_B$ is large and the TCP ($T_{TCP} = 24$ K, $P_{TCP} = 1.42$ GPa) and the QCEP ($P_{QCEP} \approx 3.5$ GPa, $H_{QCEP} \approx 18$ T) are accessible with present laboratory equipments. Fig. 7 shows the phase diagram of UGe$_2$ for $H \parallel M_0$. The (T_x, P_x) line terminates at a critical point in the $H = 0$ plane. UGe$_2$ switches from FM2 to FM1 at $H = H_x$ and from PM to FM1 at H_c. Both fields H_c and H_x will end
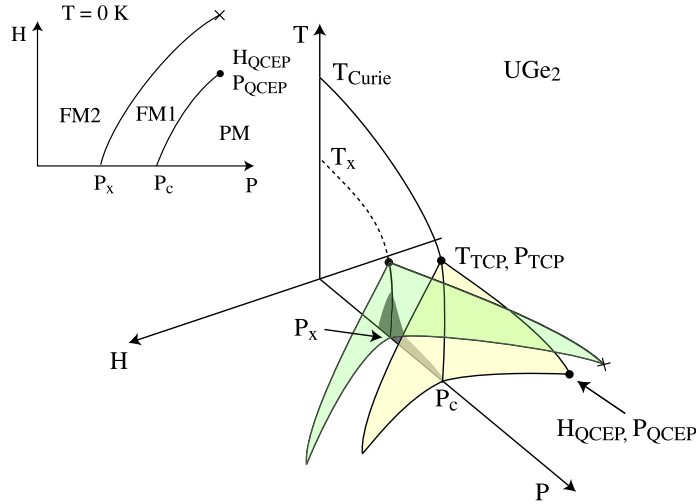
Fig. 7. Schematic (T, P, H) phase diagram of UGe$_2$. The insert shows the (H, P) plane at $T = 0$. Very recent experiments allow us to locate the position of the QCEP for H_c. The QCEP for H_x requires a new set of high field measurements.
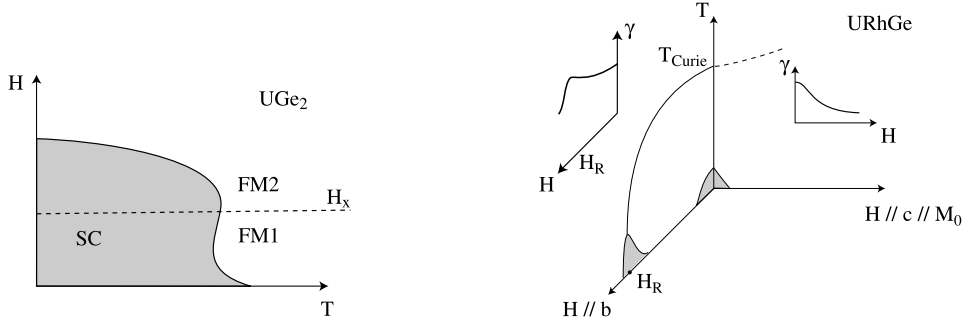

Fig. 8. Schematic temperature dependence of the upper critical field H_{c2} of UGe$_2$ for $H \parallel M_0$ (a-axis).

Fig. 9. Schematic (T, H) phase diagram for $H \parallel b$ (hard-axis) and $H \parallel c$ (easy-axis). The field dependence of γ is also depicted for both cases.

at a QCEP. High magnetic field measurements, $H > 20$ T, are necessary to clarify the QCEP for H_c. The transition from FM1 to FM2 that occurs at H_x has a strong feedback on SC as illustrated by the unusual temperature dependence of $H_{c2}(T)$ (see Fig. 8) [57]. At $H = 0$, changes of the effective mass enhancement were observed at P_x and P_c, respectively. Thus, similar changes should also occur at H_c and H_x for $P_c < P < P_{QCEP}$; on approaching P_{QCEP}, H_{QCEP} well defined maximum of $m^*(H)$ must appear. An interesting point is the possible concomitant occurrence of Lifshitz transition which is associated with the topological change of Fermi surfaces [58]. This may add another feedback for the treatment of the metamagnetic transition.

For $H \parallel M_0$, a weakening of the FM correlations similar to that of UGe$_2$ at ambient pressure is observed in URhGe and UCoGe. In URhGe, the FM transition is second order at $P = 0$ and moves away from tricriticality as P is increased since $\partial T_{Curie}/\partial P > 0$. For UCoGe, as already mentioned, the PM–FM transition may be first order [59]. However, M_0 is already weak at ambient pressure and it decreases with P. It is thus suspected that P_{QCEP} will be very close to P_c and that H_{QCEP} will be rather low.

However, spectacular effects arise for $H \perp M_0$. The transverse response leads to a decrease of T_{Curie}, which can be described using the Landau free energy [60]. Fig. 9 shows schematically the field variation of $T_{Curie}(H)$ and $\gamma(H)$ for $H \parallel M_0$ and $H \perp M_0$ in URhGe. If γ goes through a maximum, a field enhancement of m^{**} accompanied by an enhancement of T_{sc} occurs when the induced transverse magnetic component along the hard axis, *e.g.* $\chi_b H_b$ along b-axis, becomes comparable to M_0 (where χ_b is the initial slope of magnetization along b axis). Table 4 gives the estimated characteristic fields along the three axes for the three uranium SC ferromagnets.

7. Reinforcement of SC in the transverse response

In URhGe, the susceptibility along the hard magnetization axis b, $\chi_b = \partial M_b/\partial H$, is large in comparison with the easy axis c ($\chi_b/\chi_c \sim 3$). At a field $H_R \parallel b$, a reorientation of the magnetic moment occurs and the easy axis changes from the c- to the b-axis. In a restricted field range centered around H_R, reentrant SC appears. Fig. 10 shows schematic magnetization curves and the temperature dependence of M at different fields $H \parallel b$-axis. T_{Curie} is marked by a maximum of χ_b. The coefficient of the magnetization T^2 term is linked to the Sommerfeld coefficient, according to the thermodynamic Maxwell

Table 4
Susceptibilities and characteristic fields of UGe$_2$, URhGe and UCoGe.

	χ_a	χ_b (μ_B/T)	χ_c	H_a	H_b (T)	H_c
UGe$_2$	0.006	0.0055	0.011	230	250	122
URhGe	0.006	0.03	0.01	66	13	40
UCoGe	0.0024	0.006	0.029	29	12	2.5
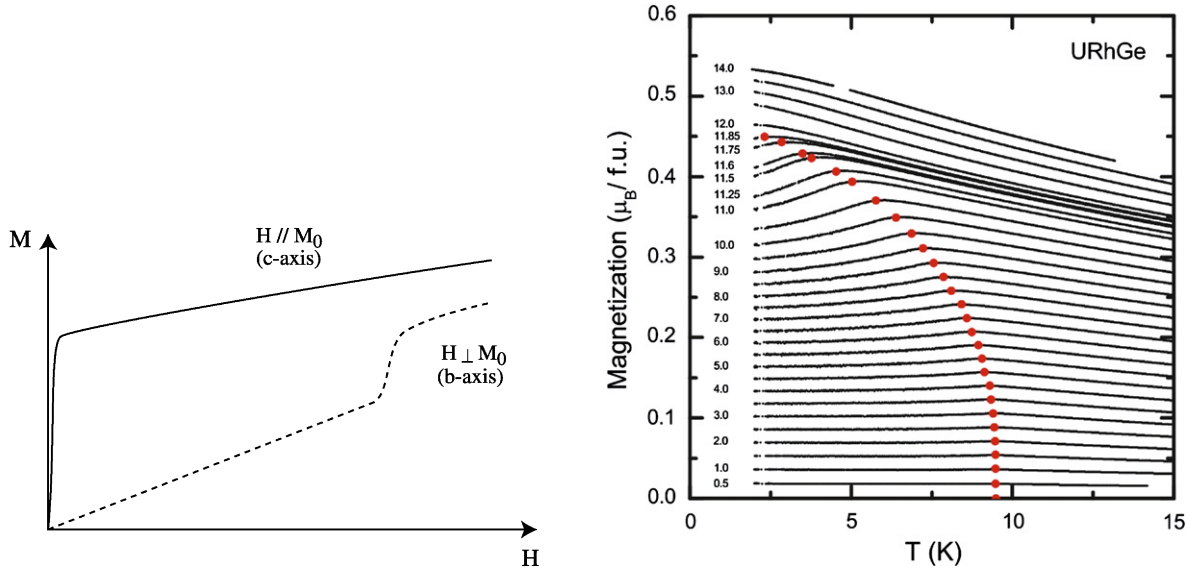
Fig. 10. Schematic magnetization curves at low temperature and the temperature dependence of magnetization at constant fields $H \parallel b$-axis in URhGe [39].
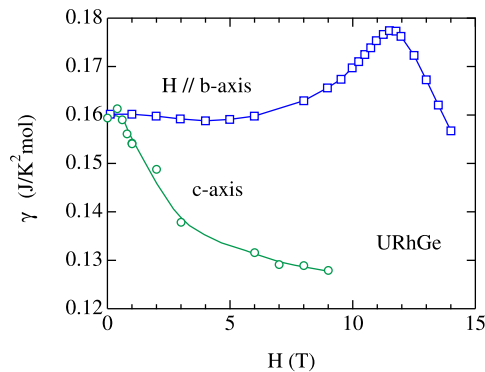

Fig. 11. Field dependence of the Sommerfeld coefficient γ obtained from the Maxwell relation (b-axis) and direct specific-heat measurements at 0.4 K (c-axis) in URhGe [39,7].

relation $\partial \gamma / \partial H = \partial^2 M / \partial T^2$. As shown here, T_{Curie} decreases with increasing field and is suppressed at H_R at low temperatures. The field dependence of the effective mass $m^*(H)$ obtained from the Maxwell relation and direct specific-heat measurements are shown in Fig. 11. The enhancement of the effective mass with increasing field $H \parallel b$ is at the origin of the reentrant SC (RSC) illustrated in Fig. 12. Using the simple formula, $T_{\text{sc}} \sim T_0 \exp(-m^*/m^{**})$, H_{c2} can be calculated within the orbital limit: $H_{c2} \sim (m^* T_{\text{sc}})^2$. Excellent agreement is obtained for the magnetic field range where RSC is observed (Fig. 13). Moreover, knowing the P dependence of $m^*(H)$, RSC is predicted to collapse at $P_{\text{RSC}} \sim 2$ GPa as observed experimentally [54].

At 0 K, we notice that a linear extrapolation of $M(H)$, for $H \parallel b$, from $H > H_R$ to $H = 0$ exhibits a non-zero intercept, suggesting that the reorientation process does not correspond to a transition to the PM regime. The preservation of the FM phase suggests that the FM Fermi surface is rather robust during the reorientation process, in good agreement with the weak singularities of the thermoelectric power detected at H_R [61].

In UCoGe, for the same field strength, no reorientation is expected since χ_c is larger than χ_b and χ_a. However, the transverse response, when H reaches H_b, leads to an unusual dependence of $H_{c2}(T)$ (as shown in Fig. 13). It is related to
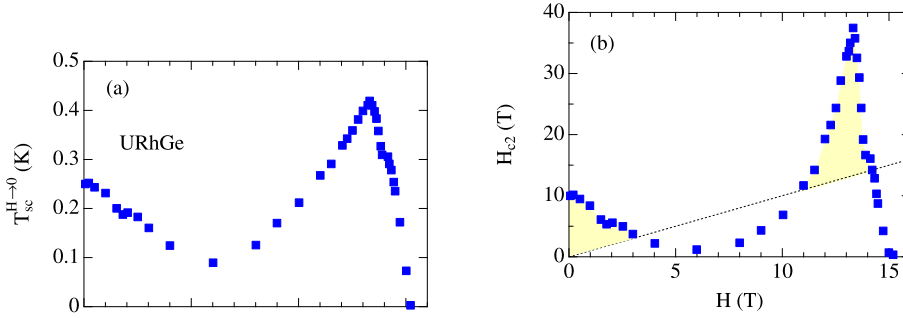
Fig. 12. Calculated T_{sc} and H_{c2} based on the field dependence of m^* in URhGe [13].
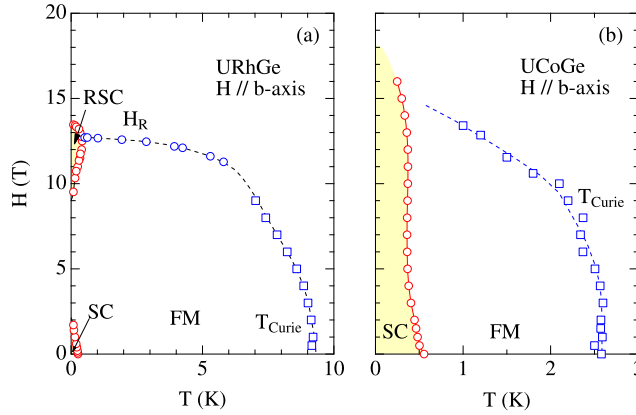

Fig. 13. (H, T) phase diagrams of URhGe and UCoGe for $H \parallel b$-axis [7,6].
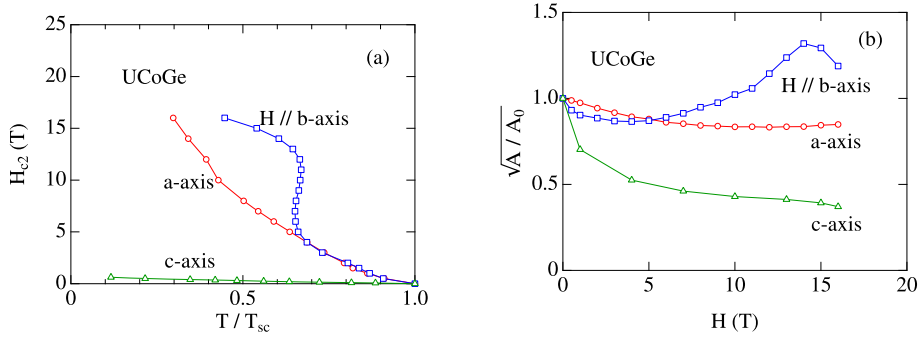

Fig. 14. (a) Temperature dependence of H_{c2} along the orthorhombic directions of UCoGe. (b) Field dependence of effective mass (the normalized $\sqrt{A}$) [6].

a field enhancement of m^* as reflected by the enhancement of $A(H)$ for $H \parallel b$ when H approaches H_b. For $H \parallel c$ a strong decrease of A is detected (Fig. 14). The calculated Fermi surface of UCoGe in the FM phase is quite different from that in the PM phase, [45] and the system is close to an FM–PM instability. Hence, it could be possible that the transverse magnetic field drives the system through the FM–PM singularity. Evidence could be given by the recent observation of large variations of the thermoelectric power at H_b [61]. In recent Shubnikov–de Haas experiments that measure the Fermi surface and the cyclotron effective mass, a quite large H response is detected [62].

8. Conclusion and remarks

We have presented the (T, P, H) phase diagrams of the three uranium ferromagnetic superconductors, UGe$_2$, URhGe and UCoGe. We have focused on the enhancement of effective mass and its relation to SC. We emphasize that the magnetic singularities at P_c, P_x, H_x, and H_c are often associated with a Fermi surface reconstruction related to the first-order nature of the magnetic transition in UGe$_2$ and UCoGe. The full determination of the Fermi surface, as a function of P and H, is expected soon thanks to progresses in the crystal purity. The case of URhGe which is located far from FM–PM instability and far from tricriticality seems to be the ideal example of FM superconductivity.

An interesting aspect of FM superconductivity concerns the influence of FM on macroscopic phenomena such as the Meissner effect [63]. Other topics are SC in FM domain walls and the phenomena associated with the relative orientation of the SC order parameter to the magnetization, the effect of SC on FM domain structure [64]. Of course as the internal field is large with respect to the lower critical field H_{c1} ($\sim 10^{-3}$ T), spontaneous vortex formation may already occur at $H = 0$. It is only recently that careful DC magnetization measurement were realized in the case of UCoGe ($4\pi M \sim 0.01$ T), no full Meissner effect, i.e. no indication of H_{c1} was detected at least for $H \parallel c$-axis. [65,66].

Advances in the field have been mainly achieved through the discovery of new systems. Even now the main goal is to discover a very clean system like Ce-115 heavy fermion superconductors where large and pure single crystals are easily available. Unfortunately up to now, high quality single crystal growth of UCoGe and URhGe is a difficult task and for UGe$_2$ SC appears only under pressure squeezed between two first-order transitions. It is worthwhile to remark that SC in FM materials has only been detected in uranium intermetallic compounds with Ising type FM, confirming the key role of longitudinal fluctuation and for materials with quite moderate heavy fermion character ($\gamma \leqslant 160$ mJ/K^2 mol) by comparison to the large value of γ (> 1 J/K^2 mol) reported for prototype d-wave superconductors (CeCu$_2$Si$_2$, Ce-115) close to their AF–PM instability. Maybe due to the low value of T_{sc} provided by FM longitudinal fluctuations and the sensitivity to disorder at both FM and SC onsets, a moderate renormalized band width is a quite favorable condition for the coexistence of FM and SC. Up to now, all attempts to discover SC in other FM materials have failed with Ce ferromagnetic heavy fermion compounds.

Acknowledgements

References

[1] S.S. Saxena, P. Agarwal, K. Ahilan, F.M. Grosche, R.K.W. Haselwimmer, M.J. Steiner, E. Pugh, I.R. Walker, S.R. Julian, P. Monthoux, G.G. Lonzarich, A. Huxley, I. Sheikin, D. Braithwaite, J. Flouquet, Nature 406 (2000) 587.
[2] D. Aoki, A. Huxley, E. Ressouche, D. Braithwaite, J. Flouquet, J.-P. Brison, E. Lhotel, C. Paulsen, Nature 413 (2001) 613.
[3] N.T. Huy, A. Gasparini, D.E. de Nijs, Y. Huang, J.C.P. Klaasse, T. Gortenmulder, A. de Visser, A. Hamann, T. Görlach, H.v. Löhneysen, Phys. Rev. Lett. 99 (2007) 067006.
[4] D. Aoki, J. Flouquet, J. Phys. Soc. Jpn., submitted for publication.
[5] F. Lévy, I. Sheikin, B. Grenier, A.D. Huxley, Science 309 (2005) 1343.
[6] D. Aoki, T.D. Matsuda, V. Taufour, E. Hassinger, G. Knebel, J. Flouquet, J. Phys. Soc. Jpn. 78 (2009) 113709.
[7] D. Aoki, T.D. Matsuda, F. Hardy, C. Meingast, V. Taufour, E. Hassinger, I. Sheikin, C. Paulsen, G. Knebel, H. Kotegawa, J. Flouquet, arXiv:1012.1987v1.
[8] A.J. Millis, Phys. Rev. B 48 (1993) 7183.
[9] J. Flouquet, in: W.P. Halperin (Ed.), Progress in Low Temperature Physics, Elsevier, Amsterdam, 2006, p. 139.
[10] M. Uhlarz, C. Pfleiderer, S.M. Hayden, Phys. Rev. Lett. 93 (2004) 256404.
[11] D. Belitz, T.R. Kirkpatrick, Jörg Rollbühler, Phys. Rev. Lett. 94 (2005) 247205.
[12] T. Takimoto, T. Moriya, Solid State Commun. 99 (1996) 457.
[13] A. Miyake, D. Aoki, J. Flouquet, J. Phys. Soc. Jpn. 77 (2008) 094709.
[14] J. Bardeen, L.N. Cooper, J.R. Schrieffer, Phys. Rev. 108 (1957) 1175.
[15] V.L. Ginzburg, Sov. Phys. JETP 4 (1957) 153.
[16] N.F. Berk, J.R. Schrieffer, Phys. Rev. Lett. 17 (1966) 433.
[17] S. Nakajima, Progr. Theoret. Phys. 50 (1973) 1101.
[18] W.F. Brinkman, J.W. Serene, P.W. Anderson, Phys. Rev. A 10 (1974) 2386.
[19] A.J. Leggett, Rev. Mod. Phys. 47 (1975) 331.
[20] A. Layzer, D. Fay, Int. J. Mag. 1 (1971) 135.
[21] D. Fay, J. Appel, Phys. Rev. B 22 (1980) 3173.
[22] R. Roussev, A.J. Millis, Phys. Rev. B 63 (2001) 140504.
[23] T.R. Kirkpatrick, D. Belitz, T. Vojta, R. Narayanan, Phys. Rev. Lett. 87 (2001) 127003.
[24] N.I. Karchev, K.B. Blagoev, K.S. Bedell, P.B. Littlewood, Phys. Rev. Lett. 86 (2001) 846.
[25] A.H. Nevidomskyy, Phys. Rev. Lett. 94 (2005) 097003.
[26] N. Karchev, Phys. Rev. B 77 (2008) 012405.
[27] D.V. Shopova, D.I. Uzunov, Phys. Rev. B 79 (2009) 064501.
[28] J. Linder, I.B. Sperstad, A.N. Nevidomskyy, M. Cuoco, A. Sudbø, Phys. Rev. B 77 (2008) 184511.
[29] P. Monthoux, G.G. Lonzarich, Phys. Rev. B 63 (2001) 054529.
[30] P. Monthoux, G.G. Lonzarich, Phys. Rev. B 69 (2004) 064517.
[31] K. Miyake, O. Narikiyo, J. Phys. Soc. Jpn. 71 (2002) 867.
[32] K.V. Samokhin, M.B. Walker, Phys. Rev. B 66 (2002) 024512.
[33] I.A. Fomin, JETP Lett. 74 (2001) 111.
[34] V.P. Mineev, Phys. Rev. B 66 (2002) 134504.
[35] F. Hardy, C. Meingast, V. Taufour, J. Flouquet, H.v. Löhneysen, R.A. Fisher, N.E. Phillips, A. Huxley, J.C. Lashley, Phys. Rev. B 80 (2009) 174521.
[36] C. Pfleiderer, A.D. Huxley, Phys. Rev. Lett. 89 (2002) 147005.
[37] A. Huxley, I. Sheikin, E. Ressouche, N. Kernavanois, D. Braithwaite, R. Calemczuk, J. Flouquet, Phys. Rev. B 63 (2001) 144519.
[38] N. Tateiwa, T.C. Kobayashi, K. Amaya, Y. Haga, R. Settai, Y. Ōnuki, Phys. Rev. B 69 (2004) 180513.
[39] F. Hardy, et al., in preparation.
[40] F. Hardy, A. Huxley, J. Flouquet, B. Salce, G. Knebel, D. Braithwaite, D. Aoki, M. Uhlarz, C. Pfleiderer, Physica B 359 (2005) 1111.

[41] T. Ohta, T. Hattori, K. Ishida, Y. Nakai, E. Osaki, K. Deguchi, N.K. Sato, I. Satoh, J. Phys. Soc. Jpn. 79 (2010) 023707.
[42] E. Hassinger, D. Aoki, G. Knebel, J. Flouquet, J. Phys. Soc. Jpn. 77 (2008) 073703.
[43] E. Hassinger, D. Aoki, G. Knebel, J. Flouquet, J. Phys.: Conf. Ser. 200 (2010) 012055.
[44] E. Slooten, T. Naka, A. Gasparini, Y.K. Huang, A. de Visser, Phys. Rev. Lett. 103 (2009) 097003.
[45] M. Samsel-Czekała, S. Elgazzar, P.M. Oppeneer, E. Talik, W. Walerczyk, R. Troć, J. Phys.: Condens. Matter 22 (2010) 015503.
[46] K. Prokeš, A. de Visser, Y.K. Huang, B. Fåk, E. Ressouche, Phys. Rev. B 81 (2010) 180407.
[47] A. Gasparini, Y.K. Huang, J. Hartbaum, H.v. Löhneysen, A. de Visser, Phys. Rev. B 82 (2010) 052502.
[48] N. Kabeya, R. Iijima, E. Osaki, S. Ban, K. Imura, K. Deguchi, N. Aso, Y. Homma, Y. Shiokawa, N. Sato, Physica B 404 (2009) 3238.
[49] S. Ban, K. Deguchi, N. Aso, Y. Homma, Y. Shiokawa, N.K. Sato, J. Magn. Magn. Mater. 310 (2007) e120.
[50] R. Settai, M. Nakashima, S. Araki, Y. Haga, T.C. Kobayashi, N. Tateiwa, H. Yamagami, Y. Ōnuki, J. Phys.: Condens. Matter 14 (2002) L29.
[51] T. Terashima, T. Matsumoto, C. Terakura, S. Uji, N. Kimura, M. Endo, T. Komatsubara, H. Aoki, Phys. Rev. Lett. 87 (2001) 166401.
[52] S. Watanabe, K. Miyake, J. Phys. Soc. Jpn. 71 (2002) 2489.
[53] K.G. Sandeman, G.G. Lonzarich, A.J. Schofield, Phys. Rev. Lett. 90 (2003) 167005.
[54] A. Miyake, D. Aoki, J. Flouquet, J. Phys. Soc. Jpn. 78 (2009) 063703.
[55] V. Taufour, D. Aoki, G. Knebel, J. Flouquet, Phys. Rev. Lett. 105 (2010) 217201.
[56] H. Kotegawa, V. Taufour, D. Aoki, G. Knebel, J. Flouquet, Phys. Rev. Lett., submitted for publication.
[57] I. Sheikin, A. Huxley, D. Braithwaite, J.P. Brison, S. Watanabe, K. Miyake, J. Flouquet, Phys. Rev. B 64 (2001) 220503.
[58] Y. Yamaji, T. Misawa, M. Imada, J. Phys. Soc. Jpn. 76 (2007) 063702.
[59] T. Ohta, Y. Nakai, Y. Ihara, K. Ishida, K. Deguchi, N.K. Sato, I. Satoh, J. Phys. Soc. Jpn. 77 (2008) 023707.
[60] V.P. Mineev, Phys. Rev. B 83 (2011) 064515.
[61] L. Malone, et al., in preparation.
[62] D. Aoki, I. Sheikin, T.D. Matsuda, V. Taufour, G. Knebel, J. Flouquet, J. Phys. Soc. Jpn. 80 (2011) 013705.
[63] D.V. Shopova, D.I. Uzunov, Phys. Rev. B 72 (2005) 024531.
[64] A.I. Buzdin, A.S. Mel'nikov, Phys. Rev. B 67 (2003) 020503.
[65] K. Deguchi, E. Osaki, S. Ban, N. Tamura, Y. Simura, T. Sakakibara, I. Satoh, N.K. Sato, J. Phys. Soc. Jpn. 79 (2010) 083708.
[66] C. Paulsen, et al., in preparation.